Zero-temperature criticality in the two-dimensional gauge glass model

Lei-Han Tang[1*] and Peiqing Tong[1,2]

[1]*Department of Physics, Hong Kong Baptist University, Kowloon Tong, Hong Kong SAR, China*
[2]*Department of Physics, Nanjing Normal University, Nanjing, Jiangsu 210097, China*
(Dated: February 2, 2008)

The zero-temperature critical state of the two-dimensional gauge glass model is investigated. It is found that low-energy vortex configurations afford a simple description in terms of gapless, weakly interacting vortex-antivortex pair excitations. A linear dielectric screening calculation is presented in a renormalization group setting that yields a power-law decay of spin-wave stiffness with distance. These properties are in agreement with low-temperature specific heat and spin-glass susceptibility data obtained in large-scale multi-canonical Monte Carlo simulations.

Rigidity is a key concept that unifies description of long-ranged order in magnets, superfluids, superconductors, and crystalline solids. [1] For two-dimensional (2D) systems with an O(2) symmetry, the helicity modulus provides a quantitative measure of rigidity, and assumes a finite value in a pure sample at sufficiently low temperatures.[2, 3] There are however a number of experimental situations, notably granular thin films of high-T_c superconductors, where one has to deal with quenched disorder that introduces random frustration and ground state vortices into the system.[4, 5, 6] Understanding how rigidity weakens or disappears altogether is crucial for interpreting the often complex equilibrium and dynamic behavior of these systems at low temperatures.[7]

The gauge glass model[8, 9] in two dimensions offers a good example where the nature of complexity and glassiness associated with strong disorder can be examined in quantitative detail. Two competing scenarios regarding the low-temperature phase diagram have been proposed: i) The system is disordered at any temperature $T > 0$, but critical at $T = 0$, as characterized by a power-law diverging glass correlation length $\xi_G \simeq T^{-\nu}$ with a rather large exponent $\nu \simeq 2.5$. [9, 10, 11, 12, 13] ii) There is a glass phase of frozen vortices that undergoes a continuous transition at $T_c \simeq 0.2J$.[14, 15, 16] Direct measurement of rigidity in terms of spin-glass susceptibility has not been able to differentiate the two scenarios unambiguously due to the relatively small system sizes examined in simulations. The domain-wall energy analysis[9] has provided some insight on the characteristics of low-lying excitations, although their true identity remains mysterious.

In this paper, we describe results of extensive numerical investigation of the 2D gauge glass model and the related Coulomb gas problem. We show that, despite strong correlation in vortex positions and the collective nature of the ground state, low energy excited states of this model take the form of a dilute gas of fermion-like vortex-antivortex pairs which have a gapless, excitation spectrum. Based on the existence of such elementary excitations, we present a phenomenological renormalization group (RG) calculation that explains the power-law decay of spin-wave stiffness $J(R) \sim R^\theta$ with distance R in the ground state. Evidence for gapless pair excitations is seen in the linear specific heat at low temperatures. The stiffness exponent θ is estimated from the strength of the screened disorder potential in the ground state of the Coulomb gas problem, and from the spin-glass susceptibility data obtained in large-scale multicanonical Monte Carlo simulations of the gauge glass model. In both cases, we obtain $\theta \simeq -0.45$, in approximate agreement with earlier studies.

The gauge glass model is defined by the Hamiltonian,

$$H = -J \sum_{\langle ij \rangle} \cos(\phi_i - \phi_j - A_{ij}), \qquad (1)$$

where ϕ_i is the phase variable on site i, J is the coupling constant, and A_{ij} are quenched random variables uniformly distributed on $[-\pi, \pi)$. Summation is over nearest neighbor pairs of sites, here on a square lattice. Decomposing the lattice gradient of the phase field ϕ_i into rotation-free and divergence-free components, one arrives at the following Coulomb gas model of vortices,[17]

$$H_v = \sum_i (m_i^2 E_c + m_i V_i) - 2\pi J \sum_{i<j} m_i m_j \ln \frac{r_{ij}}{a}. \quad (2)$$

Here m_i is the vortex charge on site i, E_c is the vortex core energy, a is the lattice constant, and r_{ij} is the distance between sites i and j. The random potential V_i can be expressed as a sum of dipolar potentials produced by the random phase shifts A_{ij}. Its statistics is specified by a logarithmically growing variance $\langle V_i^2 \rangle \simeq 2\pi\sigma J^2 \ln(L/a)$, and logarithmic spatial correlations $\langle (V_i - V_j)^2 \rangle \simeq 4\pi\sigma J^2 \ln(r_{ij}/a)$. For the gauge glass model, we have $\sigma = \pi^2/3$ and $E_c \simeq 5J$, such that approximately one third of the sites are occupied by either a vortex or an antivortex in the ground state.

Due to the high density of vortices and antivortices, the RG analysis[18, 19] developed for a dilute Coulomb gas can not be applied here. We have investigated numerically the minimal energy states of the Coulomb

gas Hamiltonian (2) using a greedy algorithm, restricting vortex charges to $m_i = 0, \pm 1$. Such states are constructed through successive addition and removal of vortex-antivortex pairs, each time picking a pair state of the lowest energy. (Note that moving a vortex to a vacant site can also be realized by such a move.) The process terminates when the system energy can not be lowered further through single pair addition or removal. In an improved ground state search, we allow the process to continue until a previous vortex configuration is revisited. Our experience shows that, for systems up to a linear size $L = 16$, the algorithm is able to find the ground state typically in 100 or fewer trials of random initial conditions.

Figure 1 illustrates results of our finding for a 16×16 system. The ground state vortex (solid circle) and antivortex (open circle) configuration $\{m_i^0\}$ is shown in Fig. 1(a). As expected, there is no apparent order of the vortices and antivortices. The same is true also for other low energy states obtained under the greedy algorithm. However, when the excess charge $\{\tilde{m}_i \equiv m_i - m_i^0\}$ of these states is plotted, as shown in Figs. 1(b)-(d), we see clearly that the low energy states overlap strongly with the ground state. The excess charges can be identified as elementary excitations that include single vortex/antivortex movement to a new position (e.g., vortex at site A to site B, vortex at site C to a neighboring site, antivortex from site G to a neighboring site, and antivortex from site H to site I), and insertion (pair D) or deletions (pairs E and F) of vortex-antivortex pairs.

Repeated numerical experiments of this type led to the following general observations: i) The ground state contains a high density of vortex-antivortex pairs of all sizes. ii) Low energy excited states can be described as a dilute gas of excess vortices from the ground state. iii) Most of the excess vortices in ii) form closely bound vortex-antivortex pairs. However, pairs of larger size [e.g., the vortex-antivortex pair at H and I in Fig. 2(d)] may also be present. They usually form a complex with smaller pairs that provide screening of the Coulomb interaction.

To characterize the energetics of low-energy pair excitations, we rewrite Eq. (2) in terms of the excess vortex charge $\tilde{m}_i = m_i - m_i^0$,

$$H_v = E_0 + \sum_i (\tilde{m}_i^2 E_c + \tilde{m}_i \tilde{V}_i) - 2\pi J \sum_{i<j} \tilde{m}_i \tilde{m}_j \ln \frac{r_{ij}}{a}. \quad (3)$$

Here E_0 is the energy of the ground state $\{m_i^0\}$, and $\tilde{V}_i$ is an effective potential at site i that includes the original disorder potential V_i as well as the potential produced by the ground state vortex population $\{m_i^0\}$.

In the original model, different Fourier components of the disorder potential are gaussian distributed and statistically independent of each other. Their variance is given by $\langle V(\mathbf{k}) V(-\mathbf{k}) \rangle = N\sigma(2\pi J)^2 G(\mathbf{k})$, where $N = L^2$ is the total number of sites and $G(\mathbf{k}) =$
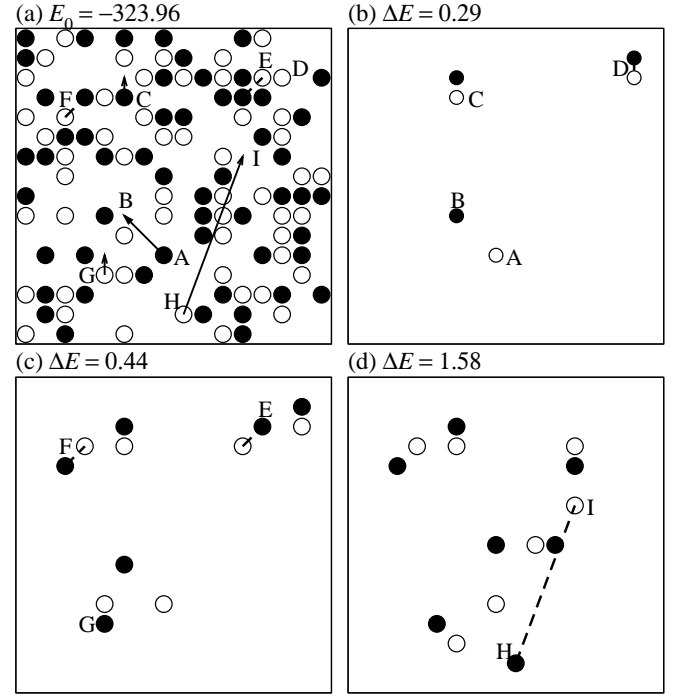

FIG. 1: (a) Vortices (solid circles) and anti-vortices (open circles) in the ground state. (b)-(d) Excited states shown in terms of excess vortices (solid circles) and antivortices (open circles) from the ground state. Energies are in units of J.

$1/[4\sin^2(k_x/2) + 4\sin^2(k_y/2)]$ is the lattice Green's function. Figure 2(a) shows $\langle \tilde{V}(\mathbf{k}) \tilde{V}(-\mathbf{k}) \rangle / G(\mathbf{k})$ at $k_y = 0$ and $k_x = 2\pi/L, 4\pi/L, \ldots, \pi$, for ground states obtained under the greedy algorithm and averaged over many disorder realizations. All energies are in units of J. Statistical errors are smaller or comparable to symbol size. It is evident that, unlike the "bare" disorder potential V_i, long wavelength components of $\tilde{V}_i$ are much reduced in strength by the ground state vortices. In fact, the data can be fitted well by assigning a $\mathbf{k}$-dependent coupling constant $J(k_x, 0) \sim |\sin(k_x/2)|^{-\theta}$, with $\theta = -0.45$, as illustrated by the dashed line in the figure.

We have also examined the size-dependence of the gap Δ between the lowest and second lowest values of $\tilde{V}_i$ in a given disorder realization. This quantity offers a measure of the spectral density of $\tilde{V}_i$ close to its minimum value, which governs vortex movement on scale L. Figure 2(b) shows the distribution of Δ for three different system sizes, which is Poisson like. The inset shows a scaling plot of $P(\Delta)$, assuming a power-law width $\Delta_L \sim L^{-0.45}$. A nearly perfect data collapse is seen.

To explain the aforementioned behavior, we consider a dielectric screening model of vortex-antivortex pairs in a phenomenological RG setting. Let R be the running length scale in an RG scheme applied to (2), and $J(R)$ be the renormalized interaction strength after pairs of size less than R have been integrated out. In an infinite
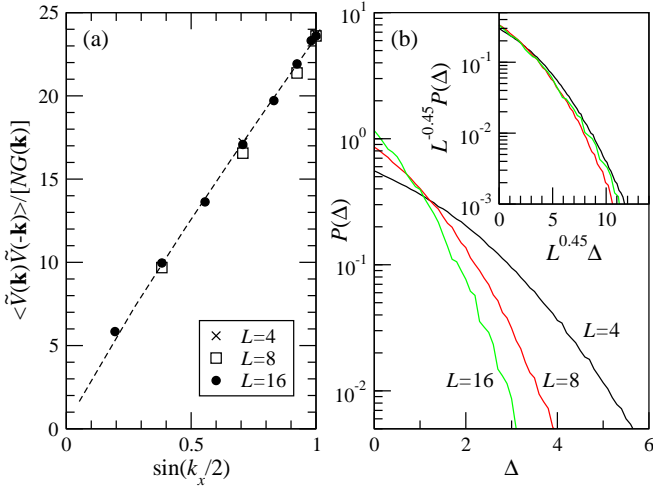
FIG. 2: (a) Scaled power spectrum of the effective disorder potential against k_x for three different system sizes. The dashed line indicates a power-law fit with an exponent $2|\theta| = 0.9$. (b) Distribution of the gap energy between the lowest and second lowest values of the effective potential. Inset shows the scaling plot of the distribution with a stiffness exponent $\theta = -0.45$.

system, the energy ϵ of pair states in the size range R to $R+dR$ forms a continuum that, for the gauge glass model, extends over both positive and negative values. Although filling of states with $\epsilon < 0$ is a collective process, the pair-pair Coulomb interaction $V_{\rm pp} \sim r^{-2}$ is not strong enough to generate a gap at the "Fermi level" $\epsilon_{\rm F} = 0$.[20] Consequently, we expect treating pairs as independent fermions is qualitatively correct. An external perturbing field $\mathbf{E}$ shifts the energy of state i by an amount $-\mathbf{E} \cdot \mathbf{p}_i$, where $\mathbf{p}_i = \mathbf{r}_i^+ - \mathbf{r}_i^-$ is the dipole moment of the pair in state i. In the neighborhood of $\epsilon_{\rm F}$, occupied and unoccupied pair states may switch under the perturbation. The induced polarization is easily calculated, from which one obtains the dielectric susceptibility for such a medium at $T = 0$,

$$\chi_R = R^2 \rho_R(0) \times (dR/R). \tag{4}$$

Here $\rho_R(0) \times (dR/R)$ is the density of pair states per unit area at $\epsilon = 0$. Let $dl = dR/R$, change in $J(R)$ due to this group of vortex-antivortex pairs can be expressed as[19],

$$dJ^{-1}/dl = 4\pi^2 \hat{\rho}(0). \tag{5}$$

where we have introduced the rescaled density of states $\hat{\rho}(0) \equiv R^2 \rho_R(0)$. Since $J(R)$ is the only energy scale at zero temperature, we may write, on dimensional grounds,

$$\hat{\rho}(0) = cJ^{-1}, \tag{6}$$

where c is some constant.[21] Combining Eqs. (5) and (6), we obtain a power-law decay of the coupling constant $J(R) = J_{\rm B} R^\theta$ in the ground state, with $\theta = -4\pi^2 c$. At a
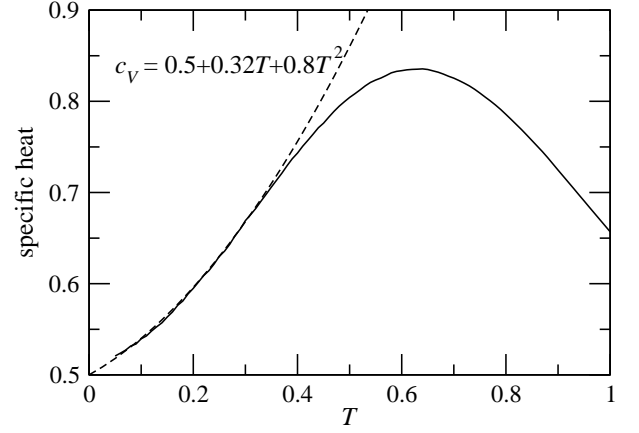
finite temperature T, Eq. (6) must be modified to take into account thermally excited pairs when one reaches a scale $\xi_{\rm G}(T)$ set by $J(\xi_{\rm G}) \simeq T$. This yields a correlation length $\xi_{\rm G} \sim T^{-1/|\theta|}$ beyond which rigidity disappears.

We have carried out extensive simulations of the gauge-glass model using a multi-canonical Monte Carlo sampling scheme that allows one to equilibrate systems of size up to $L = 48$ down to $T = 0.05$. Computation were performed on a PC cluster using up to 64 nodes. The parallel setup is ideal for calculating quantities involving the overlap $q \equiv N^{-1} \sum_j \exp[i(\phi_j^a - \phi_j^b)]$ of configurations from two different replicas a and b under the same disorder. Details of our simulation algorithm will be reported elsewhere.

Figure 3 shows the specific heat data for the $L = 48$ system, averaged over 26 disorder realizations. Comparison with data at smaller L (not shown) indicates that no significant finite-size correction is present. Data on the low temperature side can be fitted to the formula $c_V = 0.5 + 0.32T + 0.8T^2$, which has a simple physical interpretation. The constant term is due to spin-wave contributions. The linear part confirms presence of gapless vortex-antivortex pair excitations in the system.

We have also measured the $\mathbf{k}$-dependent spin-glass susceptibility

$$\chi_{\rm SG}(\mathbf{k}) = \sum_j C_{\rm SG}(r_{ij}) \exp(i\mathbf{k} \cdot \mathbf{r}_{ij}), \tag{7}$$

where $C_{\rm SG}(r_{ij}) = \langle |\overline{e^{i(\phi_i - \phi_j)}}|^2 \rangle$ is the correlation function of the glass order parameter. Here the overline bar denotes thermal average and $\langle \cdot \rangle$ denotes average over the disorder. Figure 4(a) shows $\chi_{\rm SG}(0) \equiv N \langle \overline{|q|^2} \rangle$ against T for eight different system sizes. In agreement with previous studies, the glass phase correlation grows rapidly at low temperatures. For the largest system shown at $L = 48$, crossover to finite-size dominated regime takes place already at $T \simeq 0.3$.
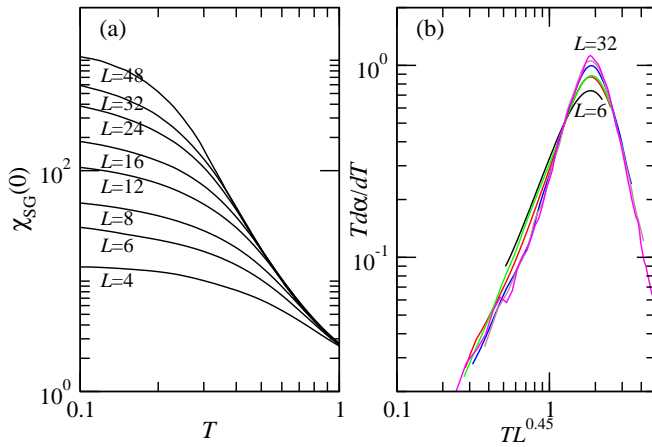

FIG. 3: Specific heat versus temperature for a 48×48 system. Dashed line shows a quadratic fit to the low temperature data.

FIG. 4: (a) Spin-glass susceptibility versus temperature for various system sizes L. (b) Temperature derivative of the susceptibility ratio at $|\mathbf{k}| = 0$ and $2\pi/L$ versus $T/J(L) = TL^{-\theta}$ for six sizes ranging from $L = 6$ to 32. See text for details.

Since spin-wave fluctuation introduces a power-law decay of $C_{SG}(r)$ at short distances with a temperature-dependent exponent $\eta(T)$, extracting $\xi_G(T)$ from the finite-size scaling ansatz[12] $\chi_{SG}(\mathbf{k}, T, L) = L^{2-\eta}\hat{\chi}(L\mathbf{k}, \xi_G/L)$ is somewhat ambiguous. Instead, one may consider the ratio $\alpha(T) \equiv \chi_{SG}(|\mathbf{k}| = 2\pi/L)/\chi_{SG}(0)$ which tends to 1 for $\xi_G \ll L$ and 0 for $\xi_G \gg L$. Crossover between the two regimes takes place at $\xi_G = L$. Figure 4(b) shows the derivative $d\alpha(T)/d\ln T$ for six different system sizes ranging from $L = 6$ to 32. The peak position of these curves yields a quantitative measure of ξ_G. Plotting the data against the scaling variable $T/J(L) = T/L^\theta$, we obtain the best collapse at $\theta = -0.45$, in agreement with the zero temperature analysis presented above.

To summarize, the picture that emerges from our study of the 2D gauge glass model is a ground state that supports gapless, fermion-like vortex-antivortex pair excitations. The energy scale of these excitations decays as a power-law of pair size — a consequence of dielectric screening by pairs of smaller size. The hierarchical organization of low energy vortices, with diminishing energy scales on increasing length scales, offers a new paradigm of zero-temperature criticality. This description is fully consistent with previous numerical work as well as our low-temperature specific heat and spin-glass susceptibility data obtained under a multicanonical Monte Carlo sampling scheme.

The composite nature of the low energy vortex-antivortex pairs of large size, with smaller and localized pairs providing screening of the long-ranged Coulomb potential, suggests possible glassy dynamic behavior. In a nonequilibrium context, the effective energy scales associated with long-distance vortex motion may be much higher than the equilibrium ones that require screening vortices to find their ideal positions. Previous simulation work on the relaxational dynamics of the gauge glass model indicates a rich behavior with multiple size-dependent time scales.[7, 13] It would be interesting to re-analyze the data in light of the new insight on the energetics of elementary vortex excitations.

* Electronic address: lhtang@hkbu.edu.hk

[1] P. W. Anderson, *Basic Notions of Condensed Matter Physics*, 2nd Ed., Westview Press, Boulder, 1997.

[2] M. E. Fisher, M. N. Barber, and D. Jasnow, Phys. Rev. A **8**, 1111 (1973).

[3] D. R. Nelson and J. M. Kosterlitz, Phys. Rev. Lett. **39**, 1201 (1977).

[4] C. Dekker, P. J. M. Wltgens, R. H. Koch, B. W. Hussey and A. Gupta, Phys. Rev. Lett. **69**, 2717 (1992).

[5] M. P. A. Fisher, Phys. Rev. Lett. **62**, 1415 (1989); D. S. Fisher, M. P. A. Fisher, and D. A. Huse, Phys. Rev. B **43**, 130 (1991).

[6] R. S. Newrock, C. J. Lobb, U. Geigenmüller, and M. Octavio, in *Solid State Physics*, Vol. 54, edited by F. Seitz *et al.* (Academic Press, New York, 2000).

[7] R. A. Hyman, M. Wallin, M. P. A. Fisher, S. M. Girvin, and A. P. Young, Phys. Rev. B **51**, 15304 (1995).

[8] C. Ebner and D. Stroud, Phys. Rev. B **31**, 165 (1985).

[9] M. P. A. Fisher, T. A. Tokuyasu and A. P. Young, Phys. Rev. Lett. **66**, 2931 (1991).

[10] J. D. Reger and A. P. Young, J. Phys. A **26**, 1067 (1993).

[11] N. Akino and J. M. Kosterlitz, Phys. Rev. B **66**, 054536 (2002).

[12] H. G. Katzgraber, Phys. Rev. B **67**, 180402(R) (2003).

[13] M. Nikolaou and M. Wallin, Phys. Rev. B **69**, 184512 (2004).

[14] M. Y. Choi and S. Y. Park, Phys. Rev. B **60**, 4070 (1999).

[15] B. J. Kim, Phys. Rev. B **62**, 644 (2000).

[16] P. Holme, B. J. Kim, and P. Minnhagen, Phys. Rev. B **67**, 104510 (2003).

[17] M. Rubinstein, B. Shraiman, and D. R. Nelson, Phys. Rev. B **27**, 1800 (1983).

[18] T. Nattermann, S. Scheidl, S. E. Korshunov, and M. S. Li, J. Phys. I (France) **5**, 565 (1995); S. E. Korshunov and T. Nattermann, Phys. Rev. B **53**, 2746 (1996); S. Scheidl, Phys. Rev. B **55**, 457 (1997).

[19] L.-H. Tang, Phys. Rev. B **54**, 3350 (1996).

[20] B. I. Shklovskii and A. L. Efros, *Electronic Properties of Doped Semiconductors* (Springer, Berlin, 1984).

[21] Eq. (6) is expected to follow from a more complete calculation which also yields a prescription for c. Such a strong-coupling theory lies outside our present scope.

Nevertheless, a case can be made for the finiteness of c by noting that pair states of negative energy in the specified size range can not exceed a few in an area R^2.

[22] B. A. Berg and T. Neuhaus, Phys. Rev. Lett. **68**, 9 (1992).